IREC
Institut de Recerca en Energia de Catalunya
Catalonia Institute for Energy Research

MANCHESTER 1824
The University of Manchester

Modelling and analysis of CIGRE HVDC offshore multi-terminal benchmark grid

Trondheim, February 2015

Jordi Pegueroles Queralt, Mike Barnes, Oriol Gomis-Bellmunt, Antony Beddard and Fernando D. Bianchi

INDEX

Motivation, 4-terminal HVDC benchamrk system by CIGRE

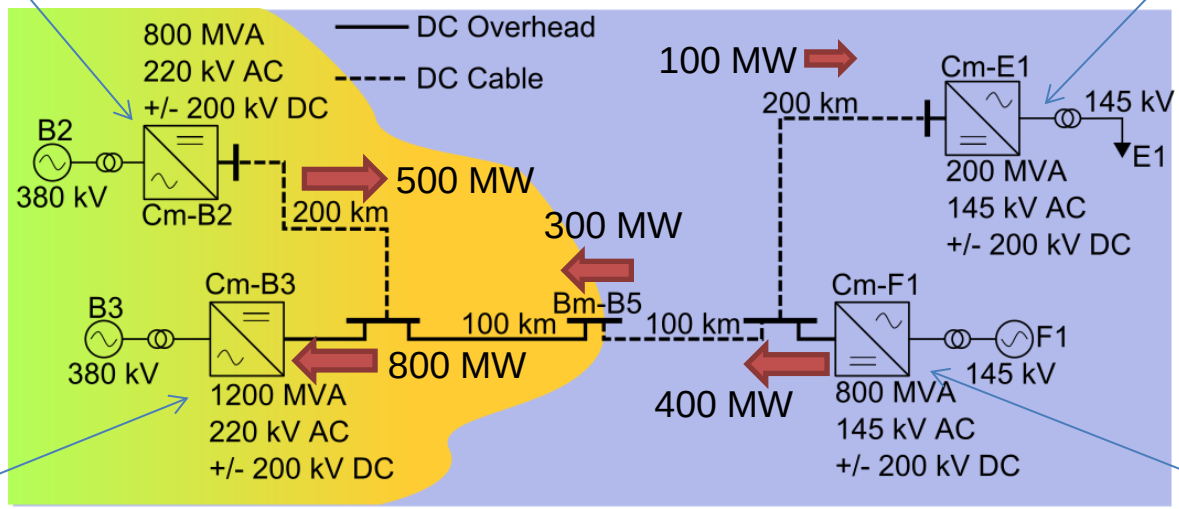

The objective is this study is to analyse of the stability and transient performance of the 4-terminal HVDC system

INDEX

Power control of HVDC converters

General control scheme for HVC converters and control loop bandwidths

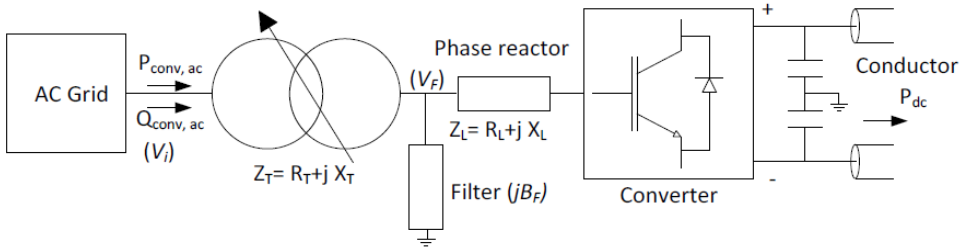

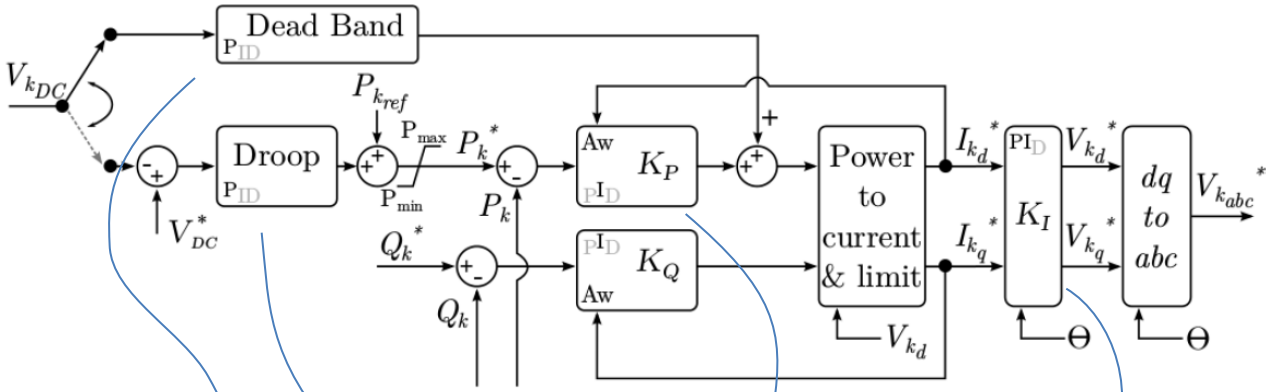

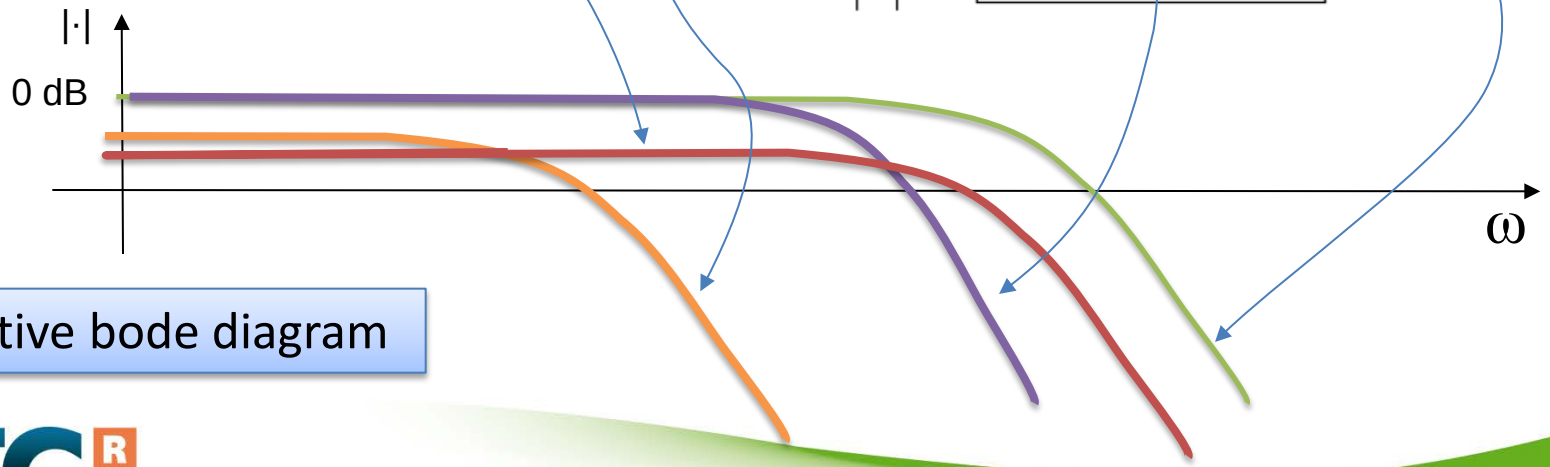

Qualitative bode diagram

Line Modelling: *n* T sections line model

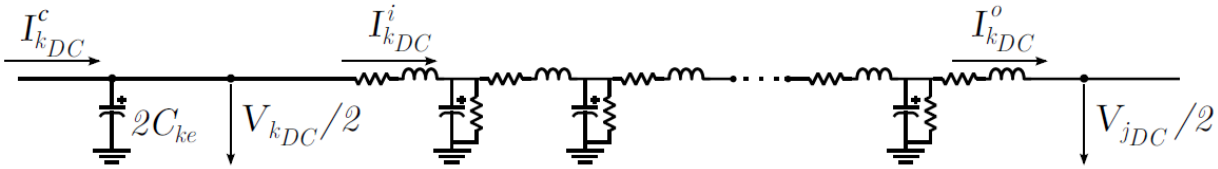

$$f_{max} = \frac{N}{\pi\Gamma\sqrt{LC}}$$

$$\frac{d}{dt}x_{line} = \Lambda_{line}x_{line} + B_{line}\Delta V_{line},$$
$$\Delta I_{line} = C_{line}x_{line}$$
$$x_{line} = \begin{bmatrix} i^1_{dc} & v^1_{dc} & i^2_{dc} & v^2_{dc} & \dots & i^{2N+1}_{dc} \end{bmatrix}^T$$

$$\Lambda = \begin{bmatrix} -\frac{r}{l} & \frac{1}{l} & 0 & 0 & 0 & \dots & 0 \\ -\frac{1}{c} & -\frac{g}{c} & \frac{1}{c} & 0 & 0 & \dots & 0 \\ 0 & -\frac{1}{l} & -\frac{r}{l} & \frac{1}{l} & 0 & \dots & 0 \\ 0 & 0 & -\frac{1}{c} & -\frac{g}{c} & \frac{1}{c} & \dots & 0 \\ \vdots & \vdots & \vdots & \ddots & \ddots & \ddots & 0 \\ 0 & 0 & 0 & 0 & 0 & -\frac{1}{l} & -\frac{r}{l} \end{bmatrix}$$

$$\Delta I_k = Y_{k\rightarrow j}\Delta V_k$$
$$\Delta I_j = Y_{k\rightarrow j}\Delta V_k$$

$$\begin{bmatrix} \Delta I_{B2_{DC}} \\ \Delta I_{B3_{DC}} \\ \Delta I_{F1_{DC}} \\ \Delta I_{E1_{DC}} \end{bmatrix} = \begin{bmatrix} Y_{B2\rightarrow B3} & -Y_{B3\rightarrow B2} & 0 & 0 \\ -Y_{B2\rightarrow B3} & Y_{B3\rightarrow B2} + Y_{B3\rightarrow F1} & -Y_{F1\rightarrow B3} & 0 \\ 0 & -Y_{B3\rightarrow F1} & Y_{F1\rightarrow B3} + Y_{F1\rightarrow E1} & -Y_{E1\rightarrow F1} \\ 0 & 0 & -Y_{F1\rightarrow E1} & Y_{E1\rightarrow F1} \end{bmatrix} \begin{bmatrix} \Delta V_{B2_{DC}} \\ \Delta V_{B3_{DC}} \\ \Delta V_{F1_{DC}} \\ \Delta V_{E1_{DC}} \end{bmatrix}$$

4 input / 4 output DC-Grid

HVDC line model

	CIGRE	used values	
Resistance	0.0110	0.0113	Ω/km
Inductance	2.6150	0.4660	mH/km
Capacitance	0.2185	0.2800	μF/km
Conductance	0.0550	0.0550	S/km

Analysing the physical specifications of the cable, and taking into account the presence of a return line, we have concluded that a slightly modified values from the ones used in the CIGRE model are more accurate for the study.

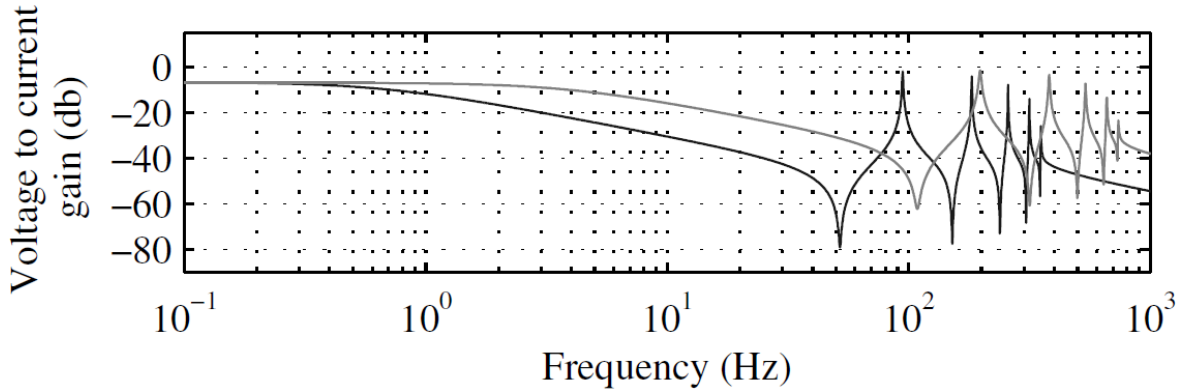

The dynamics of the line are comparable with the dynamics of the converters

INDEX

AC and DC small signal models

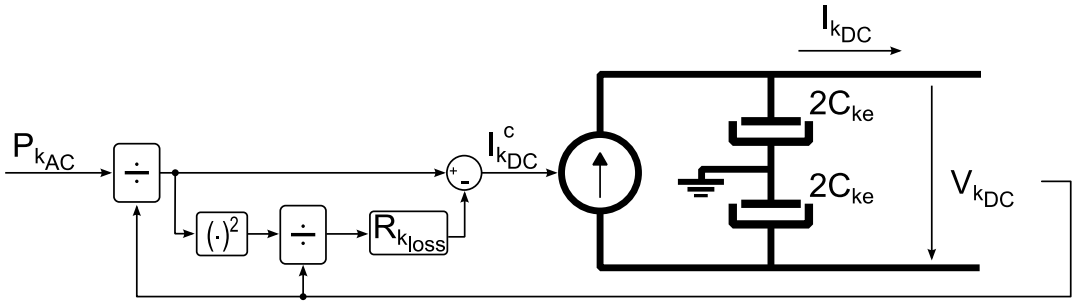

$$\Delta V_{k_{DC}} = \frac{1}{sC_{k_e}} \left(\Upsilon \Delta P_{k_{AC}} - \Delta I_{k_{DC}} \right),$$

$$\Upsilon = \frac{\frac{1}{\overline{V_{k_{DC}}}} + 2R_{k_{loss}} \overline{P_{k_{AC}}}}{1 + \frac{1}{sC_{k_e}} \left(\frac{\overline{P_{k_{AC}}}}{\overline{V_{k_{DC}}^2}} + \frac{3R_{k_{loss}} \overline{P_{k_{AC}}}}{\overline{V_{k_{DC}}^4}} \right)}$$

$$x_{ac}^{cl} = \Lambda_{ac}^{cl} x_{ac}^{cl} + \begin{bmatrix} 0 & \dots & 0 & ki_p & 0 \end{bmatrix}^T \Delta P_{k_{AC}}^*,$$

$$\Delta P_{k_{AC}} = \begin{bmatrix} \frac{3}{2}\overline{V_{k_d}} & \frac{3}{2}\overline{V_{k_q}} & 0 & \dots & 0 \end{bmatrix} x_{ac}^{cl},$$

$$\Lambda_{ac}^{cl} = \begin{bmatrix} -\frac{R_{ac}+kp_c}{L_{ac}} & 0 & \frac{1}{L_{ac}} & 0 & \frac{kp_c}{\overline{V_{k_d}}} & 0 \\ 0 & -\frac{R_{ac}+kp_c}{L_{ac}} & 0 & \frac{1}{L_{ac}} & 0 & \frac{kp_c}{\overline{V_{k_d}}} \\ -ki_c & 0 & 0 & 0 & \frac{ki_c}{\overline{V_{k_d}}} & 0 \\ 0 & -ki_c & 0 & 0 & 0 & \frac{ki_c}{\overline{V_{k_d}}} \\ -\frac{3}{2}\overline{V_{k_d}} & -\frac{3}{2}\overline{V_{k_q}} & 0 & 0 & 0 & 0 \\ -\frac{3}{2}\overline{V_{k_q}} & \frac{3}{2}\overline{V_{k_d}} & 0 & 0 & 0 & 0 \end{bmatrix}$$

VSC_k

$G\text{-}AC_k$ + $DC\text{-}Grid$

$MT\text{-}HVDC\ grid$

Sigma plot of the MT-HVDC system

MT-HVDC grid

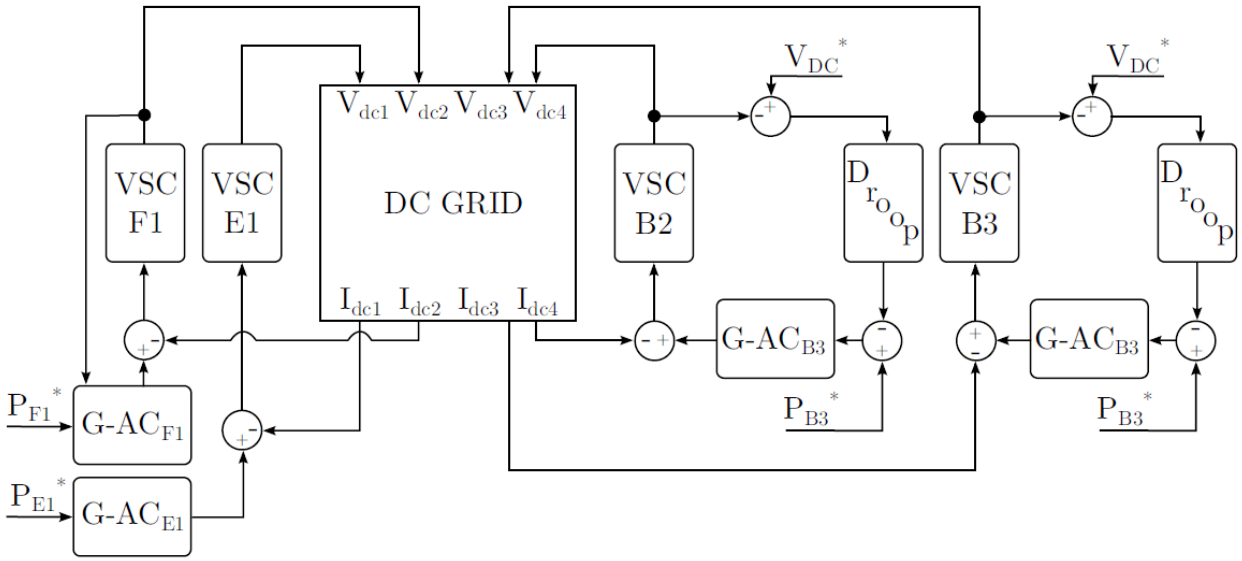

Normal operation

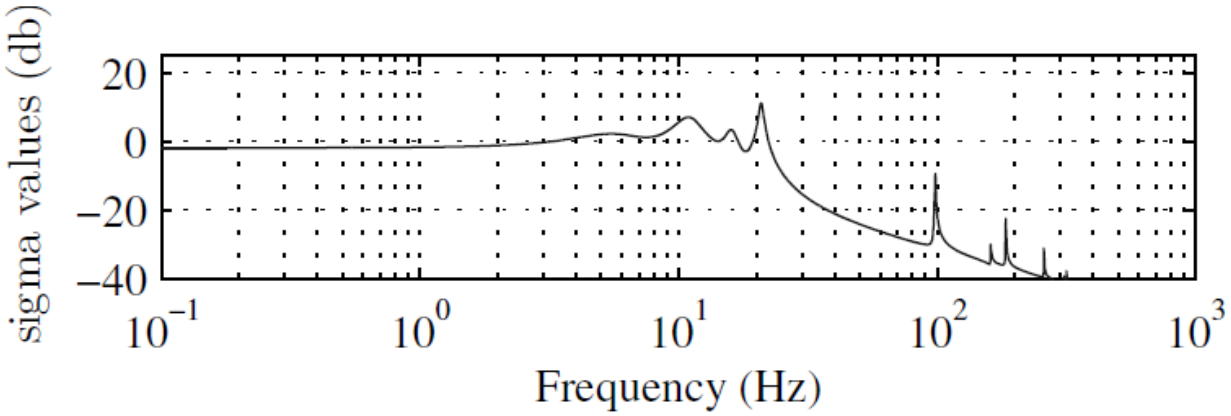

Sigma plot of the MT-HVDC system

MT-HVDC grid

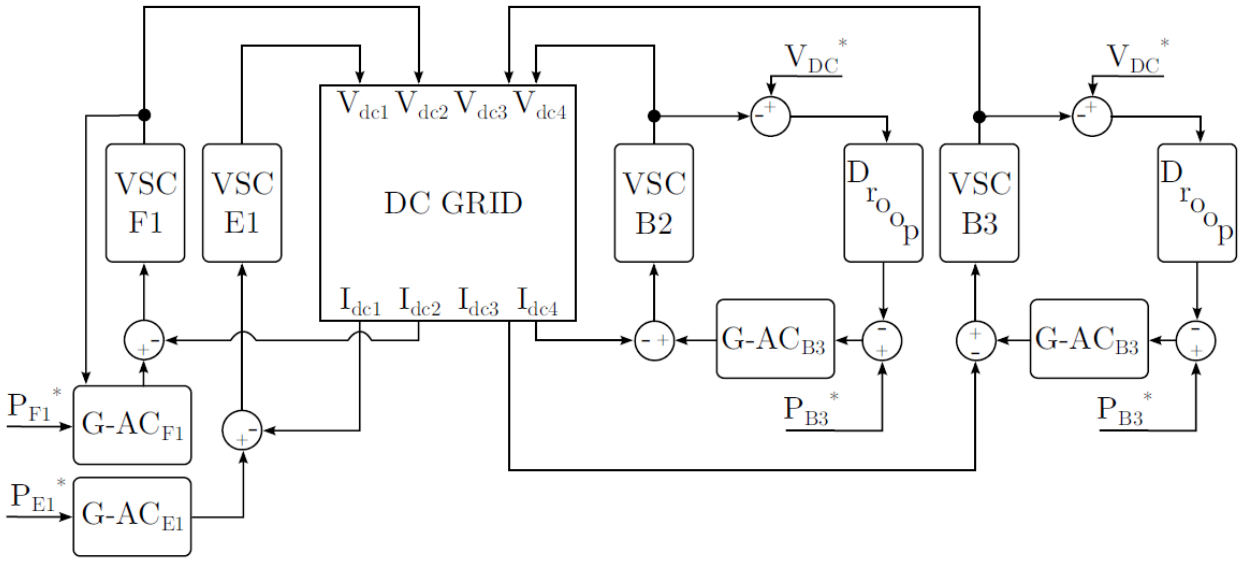

Dead band operation on the offshore wind farm

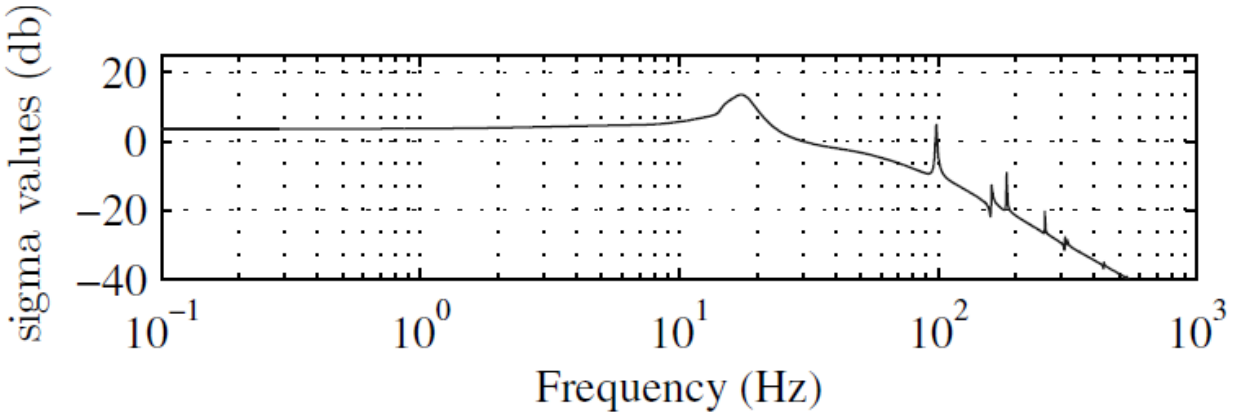

Pole location of the MT-HVDC system

MT-HVDC grid

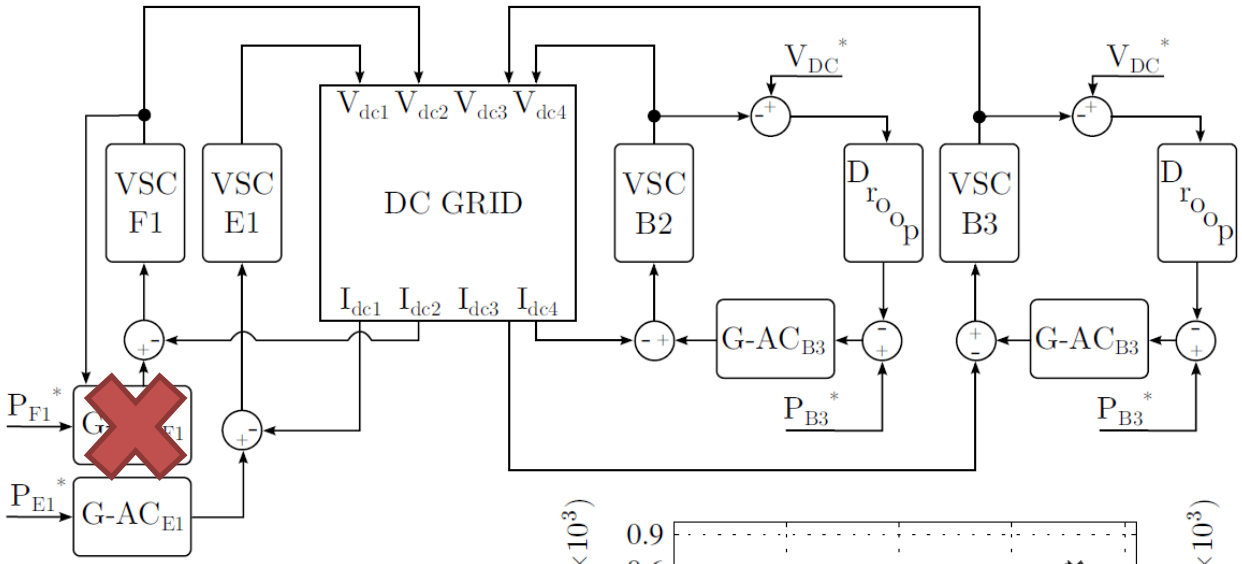

Dominant poles of the closed loop system

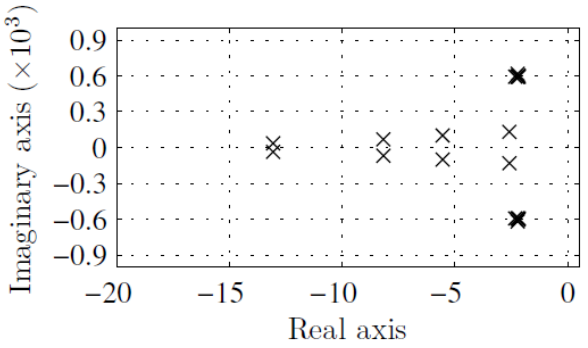

(a) With AC side of Cm-F1 converter blocked.

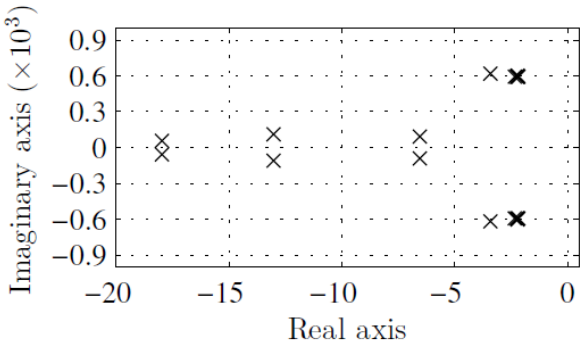

(b) With AC side of Cm-B3 converter blocked.

Pole location of the MT-HVDC system

MT-HVDC grid

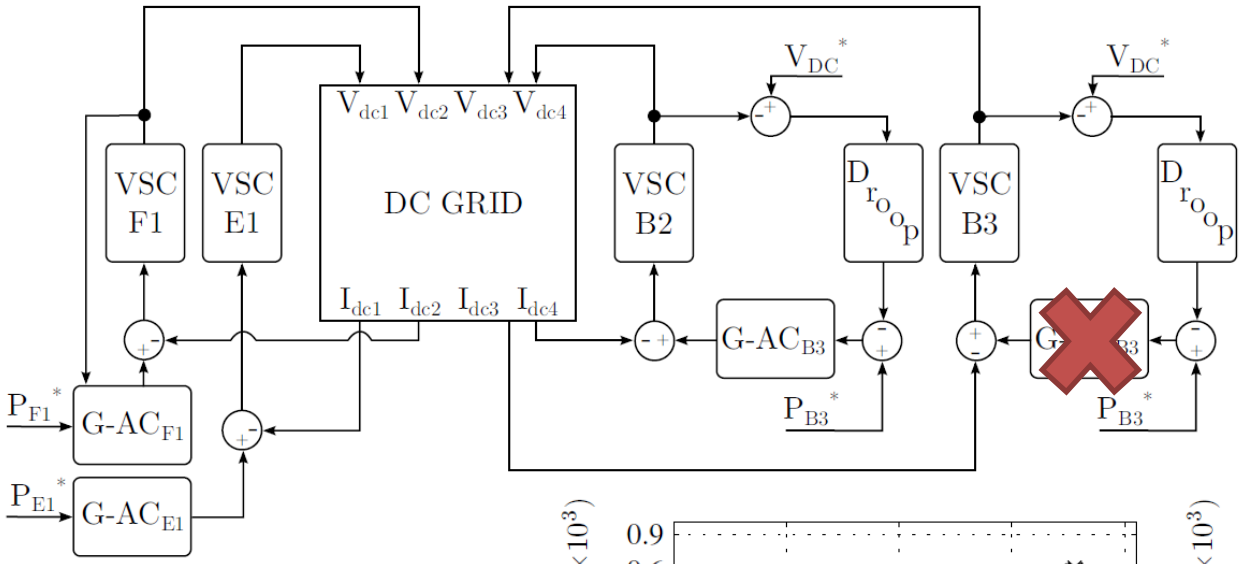

Dominant poles of the closed loop system

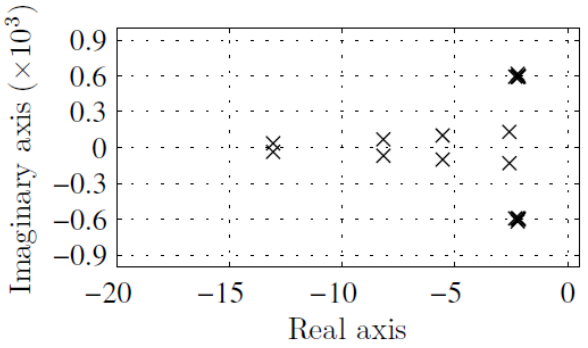

(a) With AC side of Cm-F1 converter blocked.

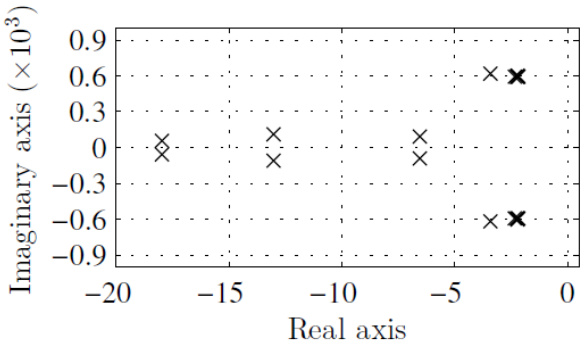

(b) With AC side of Cm-B3 converter blocked.

INDEX

Conclusions

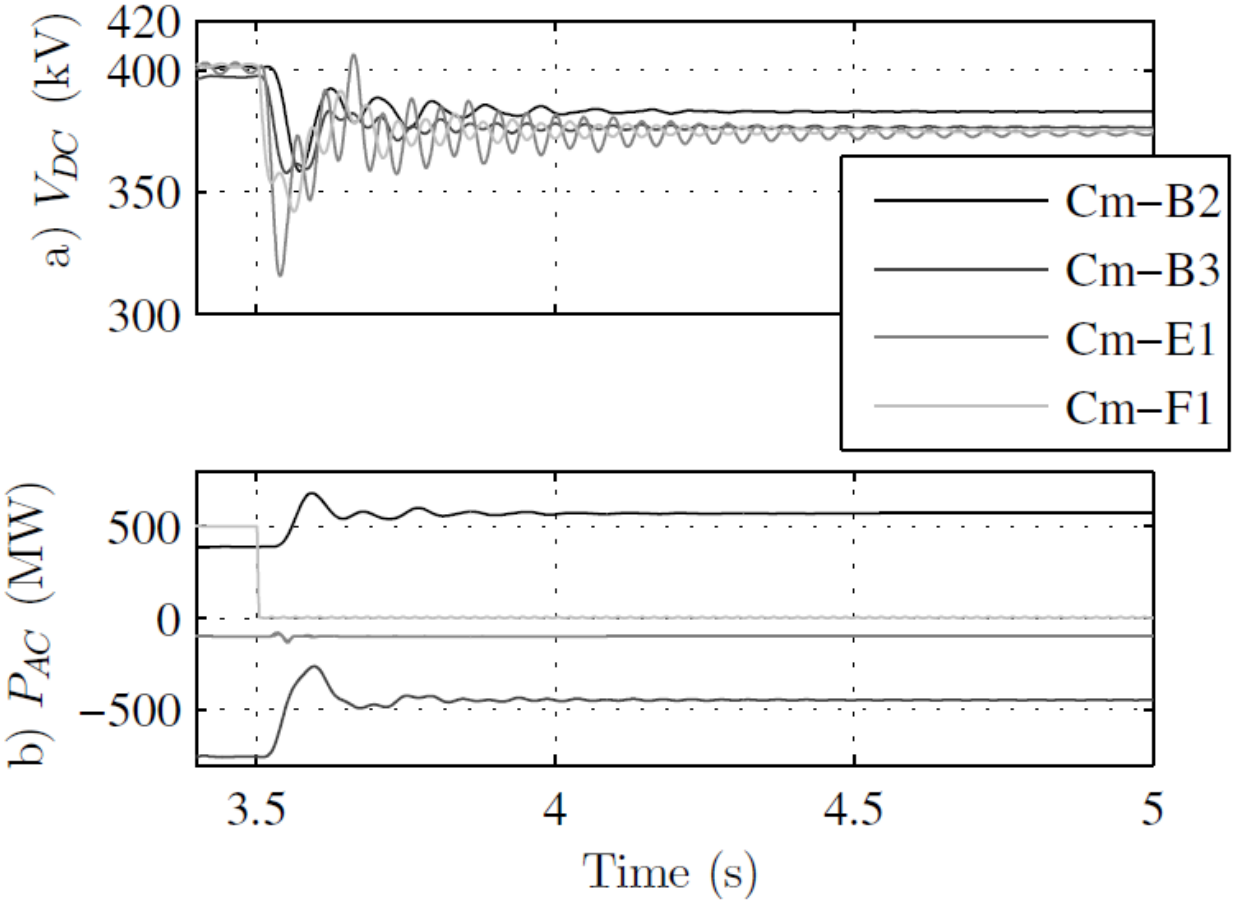

Fig. 11: Response upon the loss of Cm-F1; 2 Droop controllers

The MT-HVDC system is stable, but the interaction among the droop controllers presents a oscillatory response in the DC voltage variation, as well as on the power output

Conclusions

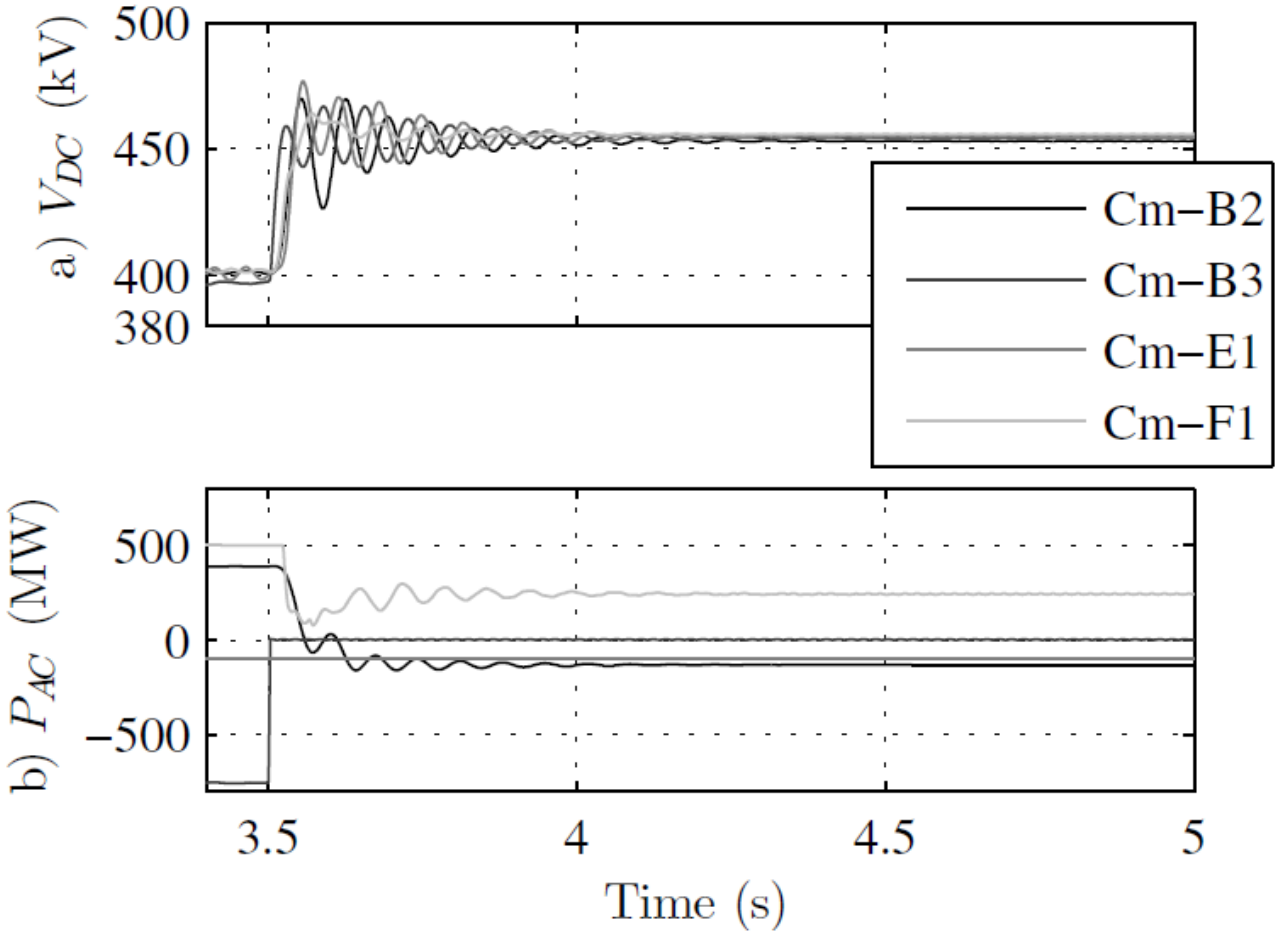

Fig. 12: Response upon the loss of Cm-B3; only one droop controller

The response of the MT-HVDC system without one of the droop converters presents a faster extintion rate than the previous case. This is also produced by the faster response of the DeadBand control of the OWP

INDEX

- **Motivation**
  - System Description
- **Control of HVDC converters**
  - Power Control
    - Droop control
  - Modelling components
    - DC line model
    - DC grid
- **Small signal models**
  - AC and DC dynamics
    - Dynamics with DeadBand
  - MT-HVDC dynamics
- **Simulations Results**
- **Conclusions**

Conclusions

- Careful coordination on the droop control is required, as parallel operation of droop controllers results in oscillatory response.

- The parameters and model of the HVDC cables have to be carefully chosen to match the frequency range of the study.

- The transient performance of the system can be improved with a more sophisticated droop control scheme.

Acknowledgements

Thanks for your attention!